

## Fluorescence and Phosphorescence Anisotropy from Oriented Films of Thermally Activated Delayed Fluorescence Emitters

Heather Fay Higginbotham, Marc Kenneth Etherington, and Andrew P. Monkman

*J. Phys. Chem. Lett.*, **Just Accepted Manuscript** • Publication Date (Web): 26 May 2017

Downloaded from <http://pubs.acs.org> on June 1, 2017

### Just Accepted

“Just Accepted” manuscripts have been peer-reviewed and accepted for publication. They are posted online prior to technical editing, formatting for publication and author proofing. The American Chemical Society provides “Just Accepted” as a free service to the research community to expedite the dissemination of scientific material as soon as possible after acceptance. “Just Accepted” manuscripts appear in full in PDF format accompanied by an HTML abstract. “Just Accepted” manuscripts have been fully peer reviewed, but should not be considered the official version of record. They are accessible to all readers and citable by the Digital Object Identifier (DOI®). “Just Accepted” is an optional service offered to authors. Therefore, the “Just Accepted” Web site may not include all articles that will be published in the journal. After a manuscript is technically edited and formatted, it will be removed from the “Just Accepted” Web site and published as an ASAP article. Note that technical editing may introduce minor changes to the manuscript text and/or graphics which could affect content, and all legal disclaimers and ethical guidelines that apply to the journal pertain. ACS cannot be held responsible for errors or consequences arising from the use of information contained in these “Just Accepted” manuscripts.



1  
2  
3  
4  
5  
6  
7  
8  
9  
10  
11  
12  
13  
14  
15  
16  
17  
18  
19  
20  
21  
22  
23  
24  
25  
26  
27  
28  
29  
30  
31  
32  
33  
34  
35  
36  
37  
38  
39  
40  
41  
42  
43  
44  
45  
46  
47  
48  
49  
50  
51  
52  
53  
54  
55  
56  
57  
58  
59  
60

# Fluorescence and Phosphorescence Anisotropy from Oriented Films of Thermally Activated Delayed Fluorescence Emitters.

*Heather F. Higginbotham, Marc. K. Etherington, Andrew P. Monkman\**

Department of Physics, Durham University, South Road. DH1 3LE. UK

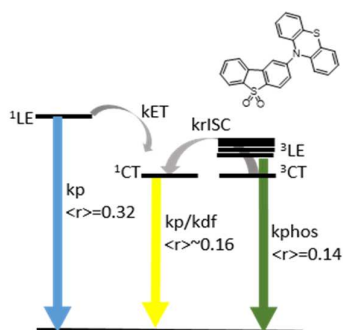
## AUTHOR INFORMATION

### **Corresponding Author**

\*a.p.monkman@durham.ac.uk

1  
2  
3 Anisotropy within three TADF materials has been observed using steady-state fluorescence  
4 polarisation. This technique has allowed for the observation of differences in polarisation  
5 within dilute solution, and both un-stretched and stretched films; the latter producing highly  
6 aligned molecules within the sample. Using these aligned films differences in anisotropy can  
7 be observed between the emission from the  $^1\text{LE}$  and  $^1\text{CT}$  states and upon exciting different  
8 absorption bands. Furthermore, polarisation observed from time-resolved measurements,  
9 highlights the strong vibronic coupling between charge-transfer and local triplet states.

## 21 TOC GRAPHICS



39 **KEYWORDS** Thermally-activated delayed fluorescence, polarisation, outcoupling, charge-  
40 transfer  
41  
42  
43  
44  
45  
46  
47  
48  
49  
50  
51  
52  
53  
54  
55  
56  
57  
58  
59  
60

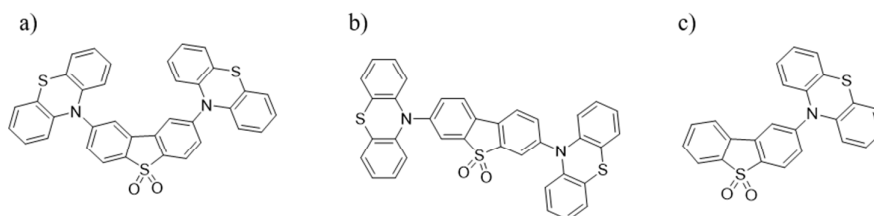
1  
2  
3 Organic light-emitting diodes (OLEDs) have come to the forefront of electronic applications  
4 due to their superior light output, colour purity and low toxicity.<sup>1,2</sup> Moreover, precise design  
5 of OLED materials has yielded compounds with internal quantum efficiency (IQE) of 100%  
6 without the use of expensive inorganic phosphor materials.<sup>3,4</sup> In many cases this has been  
7 achieved using materials capable of thermally-activated delayed fluorescence (TADF),<sup>5-8</sup>  
8 where fast reverse intersystem crossing (rISC) is capable of harvesting 100% of triplets back  
9 to emissive singlets.<sup>9,10</sup> With an abundance of OLED emitting materials exploiting TADF, a  
10 more comprehensive understanding of its mechanism is required to further knowledge of how  
11 OLED efficiency can be improved in the future.  
12  
13  
14  
15  
16  
17  
18  
19  
20  
21  
22

23  
24 As well as optimising the emitter for 100% efficient charge to light conversion, extracting  
25 light from a device is also a critical aspect of attaining an overall efficient OLED.<sup>2</sup> The  
26 process by which emission is trapped stems from how light from the emitting layer passes  
27 through further device barriers/layers of differing refractive indexes, creating total internal  
28 reflection and waveguiding within the different layers. With this in mind, the ratio of light  
29 generated internally to that which escapes the device, defines the outcoupling parameter.  
30  
31  
32  
33  
34  
35  
36

37  
38 Although outcoupling is often an overlooked parameter within device fabrication research,  
39 the term is of paramount importance when describing external quantum efficiency (EQE),  
40 arguably the most important parameter when determining OLED efficiency. With the fraction  
41 of light extracted limited to an estimated 20-30%, outcoupling therefore limits the EQE of a  
42 device to discouraging values.<sup>2,11-13</sup> The estimation of outcoupling efficiency in normal  
43 devices is based upon the assumption that within the device structure, the emitting layer  
44 contains molecules that are deposited in non-uniform orientations, creating random or  
45 isotropic emission. However research has shown that orientated emitters reduce coupling to  
46 surface plasmon modes within the interfaces of the device, increasing light extracted.<sup>14-16</sup>  
47  
48  
49  
50  
51  
52  
53  
54  
55  
56  
57  
58  
59  
60

1  
2  
3 With this knowledge in mind, there have been some investigations of molecular alignment of  
4 OLED phosphorescent<sup>16-23</sup> and TADF<sup>14,24</sup> emitters within films, using predominantly angular-  
5 dependent photoluminescence techniques in order to map the average angle of the transition  
6 dipole moment (TDM), which is fit to computational simulations. These comprehensive  
7 works, pioneered by Brütting, have shown that in some cases spontaneous horizontal  
8 molecular alignment occurs during vacuum deposition<sup>23</sup> therefore an investigation *via*  
9 artificial molecular alignment would prove an ideal model for studying light emission within  
10 a device structure.  
11  
12  
13  
14  
15  
16  
17  
18  
19

20  
21 Here we present an alternate technique to obtain the physical orientation of the TDM within a  
22 film; fluorescence polarisation spectroscopy. Using this experimental method, the relative  
23 angles between ground and excited state dipole moments can be determined, in order to map  
24 molecular anisotropy within three known TADF materials (Scheme 1). The results show that  
25 within mechanically stretched films, small organic emitters do align to give anisotropic  
26 emission and the absolute alignments of TDMs can be used to design better OLED emitting  
27 materials that can be deposited with enhancement of outcoupling in mind. It is therefore  
28 anticipated that comprehension of the TDM within TADF materials will help improve  
29 methods to increase outcoupling and assist quantum chemists in obtaining better models of  
30 molecular excited state properties.  
31  
32  
33  
34  
35  
36  
37  
38  
39  
40  
41  
42  
43  
44



**Scheme 1** Structures of three TADF emitters a) 2,8-DPTZ-DBTO<sub>2</sub> , b) 3,7-DPTZ-DBTO<sub>2</sub> and c) 2-PTZ-DBTO<sub>2</sub> used for anisotropy studies using fluorescence polarisation spectroscopy

The anisotropy a sample is determined *via* the following equation,

$$\langle r \rangle = \frac{I_{vv} - GI_{vh}}{I_{vv} + (2GI_{vh})}, \quad \text{-Equation 1}$$

where  $\langle r \rangle$  is the anisotropy of the sample,  $I_{vv}$  denotes the intensity of light with an excitation polariser and emission polariser in the vertical position,  $I_{vh}$  denotes the intensity of light obtained with the excitation polariser in the vertical and emission polariser in the perpendicular position, and  $G$  is the instrument calibration factor, which corrects for any dependencies upon polarisation within the instrument's optical components.<sup>25,26</sup> Anisotropy ( $\langle r \rangle$ ) can be related to the angle between the absorption and emission transition dipole ( $\theta$ ) *via* the following,

$$\langle r \rangle = \frac{2}{5} \frac{3\cos^2\theta - 1}{2}, \quad \text{-Equation 2}$$

where a  $\langle r \rangle$  value of 0.4 denotes complete alignment of the absorption and emission dipole moments and -0.2 denotes a 90 ° angle between the absorption and emission dipole moments. Within stretch orientated films, alignment of the absorption dipole moment with the z-axis incident light polarisation, removes the probability of photoselection observed within isotropic materials and subsequently the 2/5 parameter from the equation. This factor however remains, due to the low symmetry of the molecules, as only in highly symmetrical molecules can  $\cos^2\theta$  theoretically be 1.<sup>27</sup>

The three molecules studied, 2,8-DPTZ-DBTO<sub>2</sub>, 3,7-DPTZ-DBTO<sub>2</sub> and 2-PTZ-DBTO<sub>2</sub>, were chosen for their documented TADF properties and strong charger-transfer (CT) character, (all

1  
2  
3 of which are published by our group in the literature),<sup>9,28,29</sup> and similar structure (Scheme 1).  
4  
5 This structural similarity was chosen so that all changes in anisotropy could be attributed to  
6  
7 molecular alignment and subunit conformation, rather than dipole changes due to a change in  
8  
9 molecular structure. Absorbance of each compound in polyethylene (PE) film reproduces  
10  
11 literature results (Figure S1), with the spectra showing a characteristic absorption band in the  
12  
13 blue ( $\text{abs}_{\text{max}} \sim 340 \text{ nm}$ ), indicative of phenothiazine absorption, and a characteristic red shifted  
14  
15 ‘tail’, previously identified as direct CT absorption.<sup>28</sup> This indicates that the structural  
16  
17 integrity of the compounds is preserved even after heating and casting within the PE film.  
18  
19

20  
21 To obtain a complete picture of the anisotropy of each compound and to ensure the validity of  
22  
23 results, the compounds were analysed in dilute ( $10 \mu\text{M}$ ) toluene solution, in un-stretched PE  
24  
25 film as well as oriented films containing aligned molecules, formed through mechanical  
26  
27 stretching. Fluorescence polarisation spectroscopy of 2-PTZ-DBTO<sub>2</sub> in dilute solution shows  
28  
29 an anisotropy close to 0, indicating, not a dipole change of  $54.7^\circ$ , but the molecules’ freedom  
30  
31 to rotate on a timescale faster than the emission lifetime, resulting in emission at a large  
32  
33 distribution of angles (Figure 1a).<sup>30</sup> Solution anisotropy of 2,8-DPTZ-DBTO<sub>2</sub> and 3,7-DPTZ-  
34  
35 DBTO<sub>2</sub> show identical depolarisation effects and can be found in the supporting information  
36  
37 (Figure S2). Depolarised emission within dilute solution is indiscriminate of emitting  
38  
39 pathway from the excited state as both the <sup>1</sup>LE ( $\lambda_{\text{em}} \sim 430 \text{ nm}$ ) and <sup>1</sup>CT ( $\lambda_{\text{em}} \sim 570 \text{ nm}$ ) emission  
40  
41 in the 3,7-DPTZ-DBTO<sub>2</sub> and 2-PTZ-DBTO<sub>2</sub> samples display an anisotropy of close to 0  
42  
43 across the whole emission spectrum. The result is expected due to the low viscosity of the  
44  
45 toluene solvent and the low concentration of the solute.  
46  
47  
48  
49

50  
51 Casting 2,8-DPTZ-DBTO<sub>2</sub>, 3,7-DPTZ-DBTO<sub>2</sub> and 2-PTZ-DBTO<sub>2</sub> in solid PE film removes  
52  
53 the depolarisation due to rotation seen in dilute solutions. Regardless, the un-stretched PE  
54  
55 films also show an anisotropy of close to 0 for both <sup>1</sup>LE and <sup>1</sup>CT emission bands (Figure 1b  
56  
57  
58  
59  
60

and S3). This means that at a concentration of 1% emitter, each molecule is randomly oriented when dispersed within the film, and thus no spontaneous alignment is found. Such depolarisation proves that the estimation of the outcoupling factor in devices using these compounds, assuming random orientation, is most likely accurate and that previously reported EQEs of more than 5% can be attributed to the increase in the charge recombination parameter (due to the presence of TADF) and not an increase in outcoupling.

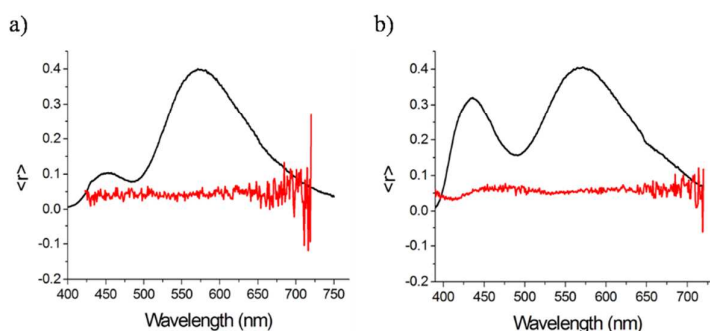


**Figure 1** a) Anisotropy of 2-PTZ-DBTO<sub>2</sub> in a) a 10  $\mu$ M toluene solution (red line) and b) an un-stretched PE film containing 1% w/w of the emitter (red line) ( $\lambda_{\text{ex}}$  370 nm). Note: The normalised emission spectrum is added in black for clarity

By stretching the film along a single axis, one can then induce molecular alignment to mimic anisotropy within an ideal OLED emissive layer. Stretched films with a stretch ratio of above 10 were analysed at different excitation wavelengths and through rotation of the film from 0-90  $^{\circ}$ ; with 0  $^{\circ}$  implying the film is placed with the stretch direction aligned with the vertically polarised excitation light, and 90  $^{\circ}$  implying that the stretch direction is perpendicular to the vertically polarised excitation light. Upon excitation at 370 nm (into the donor phenothiazine absorption band) the stretched films emit with an anisotropy related to the film orientation (Figure 2). In the 2,8-DPTZ-DBTO<sub>2</sub> film (Figure 2a), aligned with the vertical polarisation (0  $^{\circ}$ ), an anisotropy of  $0.13 \pm 0.01$  is observed for emission from the <sup>1</sup>CT state (at emission of 570 nm), a value denoting a difference between the absorption and emission dipole moment of 42



1  
2  
3 °. Rotation of the film within the holder to 20, 45, 60 and 90 °, the latter giving a  
4 perpendicular orientation of the stretch direction to the excitation polarisation, shows a  
5 reduction in anisotropy down to below 0. We observe an anisotropy specifically of 0 when  
6 the stretched film is oriented at the magic angle with respect to the light polarisation. This  
7 phenomenon is also observed in the 3,7-DPTZ-DBTO<sub>2</sub> and 2-PTZ-DBTO<sub>2</sub> samples. This loss  
8 in anisotropy is a direct result of film rotation, highlighting the alignment of the molecules  
9 within the sample.  
10  
11

12 For the 0 ° aligned films of 3,7-DPTZ-DBTO<sub>2</sub>, an anisotropy of 0.23±0.01 at 580 nm, within  
13 the <sup>1</sup>CT emission band, is observed. This value denotes an angle between the absorption and  
14 emission dipole moments of 32 °. This difference in TDM angle between the 2,8-DPTZ-  
15 DBTO<sub>2</sub> and 3,7-DPTZ-DBTO<sub>2</sub> molecules highlights the effect of different donor positioning  
16 within the two molecules and therefore the importance of molecular configuration when  
17 designing CT emitting TADF molecules, if orientation is a target parameter. The 2-PTZ-  
18 DBTO<sub>2</sub> molecule, shows CT emission with an anisotropy of 0.18±0.01 at the emission  
19 maxima of 570 nm, showing a 37 ° angle between dipole moments. Although both 2,8-  
20 DPTZ-DBTO<sub>2</sub> and 2-PTZ-DBTO<sub>2</sub> contain donor/s placed in the same position of the  
21 acceptor, the presence of a single donor in 2-PTZ-DBTO<sub>2</sub> means that its absorption and  
22 emission must come from the same donor upon each photoexcited event, unlike 2,8-DPTZ-  
23 DBTO<sub>2</sub> which may depolarise somewhat, assuming both donors are likely to photoexcite, and  
24 may indicate different orientations of each donor.<sup>29,31</sup> Local excited state (<sup>1</sup>LE) phenothiazine  
25 emission can also be seen in both the 2-PTZ-DBTO<sub>2</sub> and 3,7-DPTZ-DBTO<sub>2</sub> stretched films,  
26 with an anisotropy of 0.32±0.01 at the emission maxima of 430 nm in the former and  
27 0.41±0.03 in the latter at 0 ° film orientation. This highlights that within the dispersed host,  
28 there is no energy migration between emitter molecules and absorption and emission from  
29 <sup>1</sup>LE arises through the same orbitals. As excitation at 370 nm initially populates the local  
30  
31  
32  
33  
34  
35  
36  
37  
38  
39  
40  
41  
42  
43  
44  
45  
46  
47  
48  
49  
50  
51  
52  
53  
54  
55  
56  
57  
58  
59  
60

excited state ( $^1\text{LE}$ ) it is trivial to see that emission from the same  $^1\text{LE}$  state (at 430 nm) should induce a smaller TDM change than emission subsequently arising from the  $^1\text{CT}$  state. Furthermore, emission from both  $^1\text{LE}$  and  $^1\text{CT}$  states shows depolarisation upon film rotation and so it can be concluded that the ensemble of emitter molecules are all highly aligned.

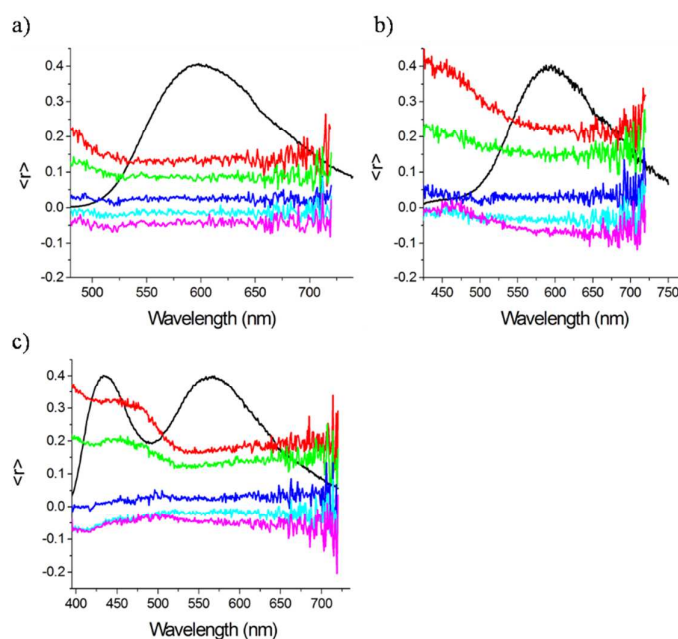


**Figure 2** Anisotropy of stretched films of 1% a) 2,8-DPTZ-DBTO<sub>2</sub> b) 3,7-DPTZ-DBTO<sub>2</sub> and c) 2-PTZ-DBTO<sub>2</sub> ( $\lambda_{\text{ex}}$  370 nm) with the stretched film aligned at 0° (red), 20° (green), 45° (blue), 60° (cyan), and 90° (pink). Note: The normalised emission spectrum is added in black for clarity

As well as probing anisotropy upon phenothiazine donor excitation, changes in polarisation can also be seen upon direct CT absorption. Dias *et al.* identified the presence of a direct CT absorbance band on the red edge (visible from  $\sim$  400-470 nm) of a UV-visible spectrum of 2,8-DPTZ-DBTO<sub>2</sub> in both film and in solution.<sup>28</sup> To further corroborate this work, stretched films of 2,8-DPTZ-DBTO<sub>2</sub>, 3,7-DPTZ-DBTO<sub>2</sub> and 2-PTZ-DBTO<sub>2</sub> were excited from 310 nm (exciting the phenothiazine donor) through to 480 nm, selectively exciting the CT absorption

1  
2  
3 band (Figure 3). Regarding 2,8-DPTZ-DBTO<sub>2</sub> with the film stretch axis aligned with the  
4  
5 vertical polarisation, the same anisotropy of  $\sim 0.14$  (for emission from the <sup>1</sup>CT state,  $\lambda_{em}$  570  
6  
7 nm) is seen when exciting the molecule between 310-370 nm, identified as excitation of the  
8  
9 phenothiazine <sup>1</sup>LE state (Figure 3a-red plot). Excitation between 390-480 nm produces a very  
10  
11 significant increase in anisotropy up to  $0.35 \pm 0.02$ , close to the maximum anisotropy and  
12  
13 denoting a difference of only  $16^\circ$  between absorption and emission dipole moments. This  
14  
15 alignment of absorption and emission dipoles clearly verifies this red edge absorption band as  
16  
17 direct CT absorption.  
18  
19

20  
21  
22 In all three molecules, the anisotropy of the un-stretched film and the dilute solutions is not  
23  
24 affected by the change in excitation wavelength, showing the same depolarisation in all cases.  
25  
26 As the un-stretched film was measured in the same holder and under identical conditions as  
27  
28 the stretched materials, it acts as an effective control for the experiment. The increase in  
29  
30 anisotropy upon change in excitation is also seen in the 3,7-DPTZ-DBTO<sub>2</sub> molecule,  
31  
32 displaying an anisotropy of  $0.42 \pm 0.04$  (when emitting from the <sup>1</sup>CT state,  $\lambda_{em}$  580 nm) when  
33  
34 excited at 480 nm, when the film is vertically aligned (Figure 3b-red plot). This value denotes  
35  
36 complete alignment of the absorption dipole moment and the emission dipole moment,  
37  
38 expected if attributed to the same CT state.  
39  
40  
41

42  
43 In all cases the anisotropy is reduced upon rotation of the film. As the film is rotated, the  
44  
45 anisotropy diminishes to below 0, further reiterating the high degree of orientation through  
46  
47 the stretching process. Interestingly, both the 3,7-DPTZ-DBTO<sub>2</sub> and 2-PTZ-DBTO<sub>2</sub> film,  
48  
49 with their two distinct emission peaks, displays discrete anisotropic behaviour for both the  
50  
51 <sup>1</sup>LE and <sup>1</sup>CT states (Figure 3c and d). In Figure 3a, b and c the presence of two absorption  
52  
53 states (<sup>1</sup>LE and <sup>1</sup>CT) is further highlighted, by monitoring the anisotropy of the CT emission  
54  
55 as a function of excitation wavelength. In Figure 3d we show the anisotropy as a function of  
56  
57  
58  
59  
60

excitation wavelength when monitoring the emission from the  $^1\text{LE}$  ( $\lambda_{\text{em}}430\text{ nm}$ ) state in 2-PTZ-DBTO<sub>2</sub>. While excitation between 310-390 nm shows no increase in the anisotropy of the CT emission, (beginning to increase only after 390 nm-Figure 3c), we observe increasing anisotropy from the  $^1\text{LE}$  emission, starting at  $0.25\pm0.02$ , at 310 nm excitation, and steadily rising to  $0.35\pm0.01$  at 390 nm excitation. Assuming that the emission dipole moment of the  $^1\text{LE}$  state is not changing (at a single film position), it again shows that there is more than one absorbing transition in this region which gives rise to  $^1\text{LE}$  emission. Emission from the locally excited state ( $\lambda_{\text{em}}430\text{ nm}$ ) is also affected by film rotation (due to the rotation of the aligned molecules and their emission dipole moment away from the excitation polarisation). We believe this is clear evidence of the mixing of  $\pi\text{-}\pi^*$  and  $\text{n-}\pi^*$  transitions in the absorption band tails as described by Marion<sup>32</sup> and in our previous work.<sup>28,33</sup>

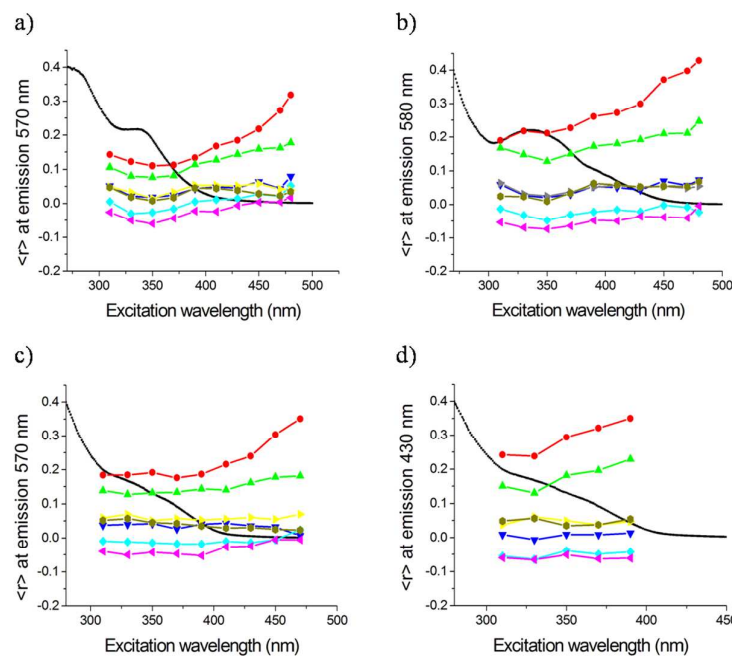


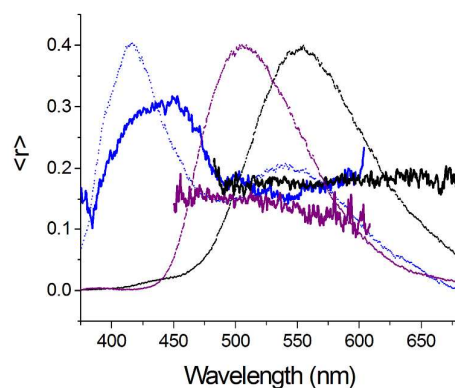
**Figure 3** Anisotropy of films of 1% a) 2,8-DPTZ-DBTO<sub>2</sub> b) 3,7-DPTZ-DBTO<sub>2</sub> and c) 2-PTZ-DBTO<sub>2</sub> with emission at 570 nm or 580 nm ( $^1\text{CT}$  emission) d) 2-PTZ-DBTO<sub>2</sub> with emission at 430 nm ( $^1\text{LE}$ ), at different excitation wavelengths, with the stretched film aligned

1  
2  
3 at 0 ° (red), 20 ° (green), 45 ° (yellow), 60 ° (cyan), 90 ° (pink), an un-stretched film (mustard)  
4  
5 and a 10 μM solution (blue). Note: The normalised excitation spectrum is added in black for  
6  
7 clarity  
8  
9

10  
11 To further characterise the position of the dipole moments within these complex molecules,  
12  
13 we turn to time-resolved anisotropy measurements. The anisotropy of 2-PTZ-DBTO<sub>2</sub> was  
14  
15 investigated in the nanosecond (prompt emission), early microsecond (TADF emission) and  
16  
17 late microsecond (phosphorescence) regions, allowing for a more comprehensive picture of  
18  
19 each TDM within this molecule (Figure S5). Polarisation was recorded using a vertically  
20  
21 polarised Nd:YAG laser, to create a polarised excitation source, coupled with a visible  
22  
23 polariser, placed after the sample in the set-up. As seen in the steady state measurements, a 2-  
24  
25 PTZ-DBTO<sub>2</sub> stretched film placed parallel (0 °) to the polarised laser produces <sup>1</sup>LE emission  
26  
27 anisotropy of 0.28±0.06 ( $\lambda_{em}$ =430 nm), with an onset of 2.98 eV and a CT anisotropy of  
28  
29 0.16±0.03 ( $\lambda_{em}$ =540 nm) at 2 ns time delay from the 0 time of the laser (Figure 4-blue plot).  
30  
31 These values are similar to those seen in steady-state spectroscopy (Figure 2c) and can thus  
32  
33 be considered as indicative of the TDM of the pure fluorescence states, <sup>1</sup>LE and <sup>1</sup>CT. At 3 μs  
34  
35 time delay, clear delayed <sup>1</sup>CT emission is observed, already fully characterised by Ward *et.*  
36  
37 *al.*, and identified as TADF. At 0 ° film alignment, this delayed emission has an anisotropy of  
38  
39 0.17±0.04, identical to the prompt <sup>1</sup>CT value within experimental error. This highlights that  
40  
41 the dipole moment of the CT state is stationary, regardless of any excursions to the triplet  
42  
43 state and back *via* rISC within the TADF mechanism. As seen in steady state polarisation  
44  
45 spectroscopy, rotation of the film depolarises the anisotropic output (Figure S6).  
46  
47  
48  
49

50  
51 At a delay time of 200 μs there is a blue shift in emission to an onset of 2.44 eV, identified as  
52  
53 emission from the triplet, <sup>3</sup>LE state. Along with this hypsochromic shift in emission,  
54  
55 manifests an additional change in anisotropy. At 0 ° film alignment, the anisotropy is reduced  
56  
57  
58  
59  
60

1  
2  
3 to  $0.14 \pm 0.04$ , therefore showing a significant change between the dipole moment position of  
4  
5 the  $^1\text{LE}$  (found at very short timescales-  $\lambda_{\text{em}} 430 \text{ nm}$ ) and the  $^3\text{LE}$  state. In contrast, the  
6  
7 phosphorescence anisotropy observed at long delay times appears similar to the anisotropy of  
8  
9 the singlet CT emission. This result is therefore surprising but not unprecedented within  
10  
11 literature. A study by Herbich *et. al.*, observed that some organic molecules displayed  
12  
13 phosphorescence anisotropy close to that of the  $^1\text{CT}$  state, not of the  $^1\text{LE}$  state.<sup>34</sup> The data  
14  
15 resulting from this literature is in line with the current model published by this group of the  
16  
17 efficient rRISC process within TADF molecules, whereby spin-orbit coupling (SOC)  
18  
19 between the  $^1\text{CT}$  state and the  $^3\text{LE}$  state (and vice versa) is mediated through  $^3\text{CT}$ - $^3\text{LE}$   
20  
21 vibronic coupling and second-order SOC.<sup>35,36</sup> These anisotropy results therefore clearly  
22  
23 suggest that the presence of strong  $^3\text{CT}$ - $^3\text{LE}$  vibronic coupling, mixes these states, resulting in  
24  
25 the observed equivalence of the  $^3\text{LE}$  and  $^1\text{CT}$  anisotropy. Therefore, this time-resolved  
26  
27 polarisation spectroscopy technique not only further corroborates the theory of  $^3\text{CT}$ - $^3\text{LE}$   
28  
29 coupling within TADF materials but can be further used as a method for identifying good  
30  
31 TADF materials in the future.  
32  
33  
34  
35  
36  
37



38  
39  
40  
41  
42  
43  
44  
45  
46  
47  
48  
49  
50  
51  
52 **Figure 4** Time resolved anisotropy of 1% 2-PTZ-DBTO<sub>2</sub> stretched film (0 °) excited at 355  
53 nm at 2 ns (blue), 3 μs (black), and 200 μs (purple). Note: The normalised emission spectrum  
54 (dashed lines) is added in blue (2 ns), black (3 μs) and purple (200 μs) for clarity  
55  
56  
57  
58  
59  
60

1  
2  
3 Polarisation spectroscopy has allowed for the identification of changes in TDM upon  
4 emission from the local and charge-transfer states. In relation to research of enhancing  
5 outcoupling, it is possible to induce TADF molecular alignment within films, allowing for the  
6 development of an accurate experimental model for dipole alignment within OLED  
7 structures, which is consistent with the observation of increased yield for outcoupled  
8 emission within devices. Nevertheless care should be taken by both experimental and  
9 computation researchers, due to the complicated excited state dynamics within these  
10 seemingly simple TADF materials. It is hoped that this and other such studies will assist  
11 quantum chemists in obtaining better models to be applied to OLED research and design.  
12  
13  
14  
15  
16  
17  
18  
19  
20  
21  
22

#### 23 ASSOCIATED CONTENT

24  
25  
26  
27 Supporting Information: The Supporting Information is available free of charge on the ACS  
28 Publications website at DOI: XXXXXXXXX. Provided are the experiment methods,  
29 absorbance spectra of films and additional anisotropy data.  
30  
31  
32

#### 33 AUTHOR INFORMATION

##### 34 **Corresponding author**

35  
36  
37 A.P.M: Email: a.p.monkman@durham.ac.uk  
38  
39  
40  
41

##### 42 **Notes**

43  
44 The authors declare no competing financial interests.  
45  
46

#### 47 ACKNOWLEDGMENT

48  
49  
50 H.F.H M.K.E and A.P.M acknowledge the EU's Horizon 2020 for funding the PHEBE  
51 project under grant no. 6,41,725.  
52  
53  
54

#### 55 REFERENCES

56  
57  
58  
59  
60

- 1  
2  
3  
4  
5 (1) Tao, Y.; Yuan, K.; Chen, T.; Xu, P.; Li, H.; Chen, R.; Zheng, C.; Zhang, L.; Huang, W.  
6  
7 Thermally Activated Delayed Fluorescence Materials Towards the Breakthrough of  
8  
9 Organoelectronics. *Adv. Mater.* **2014**, *26*, 7931–7958.  
10  
11  
12 (2) Chang, Y. L. *Efficient Organic Light-Emitting Diodes (OLEDs)*; Pan Stanford Publishing,  
13  
14 2015.  
15  
16  
17 (3) Baldo, M. A.; O'Brien, D. F.; You, Y.; Shoustikov, A.; Sibley, S.; Thompson, M. E.;  
18  
19 Forrest, S. R. Highly Efficient Phosphorescent Emission from Organic Electroluminescent  
20  
21 Devices. *Nature* **1998**, *395*, 151–154.  
22  
23  
24 (4) Baldo, M. A.; Thompson, M. E.; Forrest, S. R. High-Efficiency Fluorescent Organic  
25  
26 Light-Emitting Devices Using a Phosphorescent Sensitizer. *Nature* **2000**, *403*, 750–753.  
27  
28  
29 (5) Yang, Z.; Mao, Z.; Xie, Z.; Zhang, Y.; Liu, S.; Zhao, J.; Xu, J.; Chi, Z.; Aldred, M. P.  
30  
31 Recent Advances in Organic Thermally Activated Delayed Fluorescence Materials. *Chem.*  
32  
33 *Soc. Rev.* **2017**, *46*, 915–1016.  
34  
35  
36 (6) Uoyama, H.; Goushi, K.; Shizu, K.; Nomura, H.; Adachi, C. Highly Efficient Organic  
37  
38 Light-Emitting Diodes from Delayed Fluorescence. *Nature* **2012**, *492*, 234–238.  
39  
40  
41 (7) Zhang, Q.; Li, B.; Huang, S.; Nomura, H.; Tanaka, H.; Adachi, C. Efficient Blue Organic  
42  
43 Light-Emitting Diodes Employing Thermally Activated Delayed Fluorescence. *Nat. Photon.*  
44  
45 **2014**, *8*, 326–332.  
46  
47  
48 (8) Jankus, V.; Data, P.; Graves, D.; McGuinness, C.; Santos, J.; Bryce, M. R.; Dias, F. B.;  
49  
50 Monkman, A. P. Highly Efficient TADF OLEDs: How the Emitter–Host Interaction Controls  
51  
52  
53  
54  
55  
56  
57  
58  
59  
60



1  
2  
3 Both the Excited State Species and Electrical Properties of the Devices to Achieve Near  
4  
5 100% Triplet Harvesting and High Efficiency. *Adv. Funct. Mater.* **2014**, *24*, 6178–6186.  
6  
7

8  
9 (9) Ward, J. S.; Nobuyasu, R. S.; Batsanov, A. S.; Data, P.; Monkman, A. P.; Dias, F. B.;  
10  
11 Bryce, M. R. The Interplay of Thermally Activated Delayed Fluorescence (TADF) and Room  
12  
13 Temperature Organic Phosphorescence in Sterically-Constrained Donor-Acceptor Charge-  
14  
15 Transfer Molecules. *Chem. Commun.* **2016**, *52*, 2612–2615.  
16  
17

18  
19 (10) Dias, F. B.; Pollock, S.; Hedley, G.; Pålsson, L. O.; Monkman, A.; Perepichka, I. I.;  
20  
21 Perepichka, I. F.; Tavasli, M.; Bryce, M. R. Intramolecular Charge Transfer Assisted by  
22  
23 Conformational Changes in the Excited State of Fluorene-dibenzothiophene-S,S-dioxide Co-  
24  
25 oligomers. *J. Phys. Chem. B* **2006**, *110*, 19329–19339.  
26  
27

28  
29 (11) Gather, M. C.; Reineke, S. Recent Advances in Light Outcoupling from White Organic  
30  
31 Light-Emitting Diodes. *J. Photon. Energy* **2015**, *5*, 057607-1–057607-20.  
32  
33

34  
35 (12) Saxena, K.; Jain, V. K.; Mehta, D. S. A Review on the Light Extraction Techniques in  
36  
37 Organic Electroluminescent Devices. *Opt. Mater.* **2009**, *32*, 221–233.  
38  
39

40  
41 (13) Patel, N. K.; Cina, S.; Burroughes, J. H. High-Efficiency Organic Light-Emitting  
42  
43 Diodes. *IEEE J. Sel. Top. Quantum Electron.* **2002**, *8*, 346–361.  
44  
45

46  
47 (14) Mayr, C.; Lee, S. Y.; Schmidt, T. D.; Yasuda, T.; Adachi, C.; Brütting, W. Efficiency  
48  
49 Enhancement of Organic Light-Emitting Diodes Incorporating a Highly Oriented Thermally  
50  
51 Activated Delayed Fluorescence Emitter. *Adv. Funct. Mater.* **2014**, *24*, 5232–5239.  
52  
53

54  
55 (15) Nowy, S.; Krummacher, B. C.; Frischeisen, J.; Reinke, N. A.; Brütting, W. Light  
56  
57 Extraction and Optical Loss Mechanisms in Organic Light-Emitting Diodes: Influence of the  
58  
59 Emitter Quantum Efficiency. *J. Appl. Phys.* **2008**, *104*, 123109-1–123109-9.  
60

1  
2  
3 (16) Flämmich, M.; Frischeisen, J.; Setz, D. S.; Michaelis, D.; Krummacher, B. C.; Schmidt,  
4  
5 T. D.; Brütting, W.; Danz, N. Oriented Phosphorescent Emitters Boost OLED Efficiency.  
6  
7 *Org. Electron.* **2011**, *12*, 1663–1668.

8  
9  
10 (17) Lampe, T.; Schmidt, T. D.; Jurow, M. J.; Djurovich, P. I.; Thompson, M. E.; Brütting,  
11  
12 W. Dependence of Phosphorescent Emitter Orientation on Deposition Technique in Doped  
13  
14 Organic Films. *Chem. Mater.* **2016**, *28*, 712–715.

15  
16  
17 (18) Schmidt, T. D.; Setz, D. S.; Flämmich, M.; Frischeisen, J.; Michaelis, D.; Krummacher,  
18  
19 B. C.; Danz, N.; Brütting, W. Evidence for Non-Isotropic Emitter Orientation in a Red  
20  
21 Phosphorescent Organic Light-Emitting Diode and its Implications for Determining the  
22  
23 Emitter's Radiative Quantum Efficiency. *Appl. Phys. Lett.* **2011**, *99*, 163302-1–163302-3.

24  
25  
26 (19) Kim, K. H.; Moon, C. K.; Lee, J. H.; Kim, S. Y.; Kim, J. J. Highly Efficient Organic  
27  
28 Light-Emitting Diodes with Phosphorescent Emitters Having High Quantum Yield and  
29  
30 Horizontal Orientation of Transition Dipole Moments. *Adv. Mater.* **2014**, *26*, 3844–3847.

31  
32  
33 (20) Liehm, P.; Murawski, C.; Furno, M.; Lüssem, B.; Leo, K.; Gather, M. C. Comparing the  
34  
35 Emissive Dipole Orientation of Two Similar Phosphorescent Green Emitter Molecules in  
36  
37 Highly Efficient Organic Light-Emitting Diodes. *Appl. Phys. Lett.* **2012**, *101*, 253304-1–  
38  
39 253304-4.

40  
41  
42 (21) Kim, S. Y.; Jeong, W. I.; Mayr, C.; Park, Y. S.; Kim, K. H.; Lee, J. H.; Moon, C. K.;  
43  
44 Brütting, W.; Kim, J. J. Organic Light-Emitting Diodes with 30% External Quantum  
45  
46 Efficiency Based on a Horizontally Oriented Emitter. *Adv. Funct. Mater.* **2013**, *23*, 3896–  
47  
48 3900.

1  
2  
3 (22) Kim, K.-H.; Liao, J. L.; Lee, S. W.; Sim, B.; Moon, C. K.; Lee, G. H.; Kim, H. J.; Chi,  
4  
5 Y.; Kim, J. J. Crystal Organic Light-Emitting Diodes with Perfectly Oriented Non-Doped Pt-  
6  
7 Based Emitting Layer. *Adv. Mater.* **2016**, *28*, 2526–2532.

8  
9  
10 (23) Jurow, M. J.; Mayr, C.; Schmidt, T. D.; Lampe, T.; Djurovich, P. I.; Brutting, W.;  
11  
12 Thompson, M. E. Understanding and Predicting the Orientation of Heteroleptic Phosphors in  
13  
14 Organic Light-Emitting Materials. *Nat. Mater.* **2016**, *15*, 85–91.

15  
16  
17 (24) Sun, J. W.; Kim, K. H.; Moon, C. K.; Lee, J. H.; Kim, J. J. Highly Efficient Sky-Blue  
18  
19 Fluorescent Organic Light Emitting Diode Based on Mixed Cohost System for Thermally  
20  
21 Activated Delayed Fluorescence Emitter (2CzPN). *ACS Appl. Mater. Interf.* **2016**, *8*, 9806–  
22  
23 9810.

24  
25  
26 (25) Vaughan, H. L.; Dias, F. M. B.; Monkman, A. P. An Investigation into the Excitation  
27  
28 Migration in Polyfluorene Solutions via Temperature Dependent Fluorescence Anisotropy. *J.*  
29  
30 *Chem. Phys.* **2005**, *122*, 014902.

31  
32  
33 (26) Vaughan, H. L.; Monkman, A. P.; Pålsson, L.-O.; Nehls, B. S.; Farrell, T.; Scherf, U. On  
34  
35 the Angular Dependence of the Optical Polarization Anisotropy in Ladder-Type Polymers. *J.*  
36  
37 *Chem. Phys.* **2008**, *128*, 044709.

38  
39  
40 (27) Thulstrup, E.W. and Michl, J. Polarized Absorption Spectroscopy of Molecules Aligned  
41  
42 in Stretched Polymers. *Spectrochim. Acta* **1988**, *44A*, 767-782.

43  
44  
45 (28) Dias, F. B.; Santos, J.; Graves, D. R.; Data, P.; Nobuyasu, R. S.; Fox, M. A.; Batsanov,  
46  
47 A. S.; Palmeira, T.; Berberan-Santos, M. N.; Bryce, M. R.; Monkman, A. P. The Role of  
48  
49 Local Triplet Excited States and D-A Relative Orientation in Thermally Activated Delayed  
50  
51 Fluorescence: Photophysics and Devices. *Adv. Sci.* **2016**, *3*, 1600080.  
52  
53  
54  
55  
56  
57  
58  
59  
60

1  
2  
3 (29) Etherington, M. K.; Franchello, F.; Gibson, J.; Northey, T.; Santos, J.; Ward, J. S.; Data,  
4 P.; Kurowska, A.; Higginbotham, H. F.; dos Santos, P. L.; Graves, D. R.; Batsanov, A. S.;  
5  
6  
7 Dias, F. B.; Bryce, M. R.; Penfold, T. J.; Monkman, A. P. Regio- and Conformational  
8  
9 Isomerisation Critical to Design of Efficient Thermally-activated Delayed Fluorescence  
10  
11 Emitters. *Nat. Commun.* **2017**, *8*, 1–11.  
12

13  
14  
15 (30) Lakowicz, J. R. *Principles of Fluorescence Spectroscopy*; Springer, 2006  
16  
17

18  
19 (31) Okazaki, M.; Takeda, Y.; Data, P.; Pander, P.; Higginbotham, H.; Monkman, A. P.;  
20  
21 Minakata, S. Thermally Activated Delayed Fluorescent Phenothiazine-  
22  
23 Dibenzo[a,j]phenazine-phenothiazine Triads Exhibiting Tricolor-Changing Mechanochromic  
24  
25 Luminescence. *Chem. Sci.* **2017**, *8*, 2677–2686.  
26  
27

28  
29 (32) Marian, C. M. A New Pathway for the Rapid Decay of Electronically Excited Adenine.  
30  
31 *J. Chem. Phys.* **2005**, *122*, 104314.  
32  
33

34 (33) Dias, F. B.; Bourdakos, K. N.; Jankus, V.; Moss, K. C.; Kamtekar, K. T.; Bhalla, V.;  
35  
36 Santos, J.; Bryce, M. R.; Monkman, A. P. Triplet Harvesting with 100% Efficiency by Way  
37  
38 of Thermally Activated Delayed Fluorescence in Charge Transfer OLED Emitters. *Adv.*  
39  
40 *Mater.* **2013**, *25*, 3707–3714.  
41  
42

43  
44 (34) Herbich, J.; Kapturkiewicz, A.; Nowacki, J. Phosphorescent Intramolecular Charge  
45  
46 Transfer Triplet States. *Chem. Phys. Lett.* **1996**, *262*, 633–642.  
47  
48

49  
50 (35) Gibson, J.; Monkman, A. P.; Penfold, T. J. The Importance of Vibronic Coupling for  
51  
52 Efficient Reverse Intersystem Crossing in Thermally Activated Delayed Fluorescence  
53  
54 Molecules. *ChemPhysChem* **2016**, *17*, 2956–2961.  
55  
56  
57  
58  
59  
60

1  
2  
3 (36) Etherington, M. K.; Gibson, J.; Higginbotham, H. F.; Penfold, T. J.; Monkman, A. P.  
4  
5 Revealing the Spin-Vibronic Coupling Mechanism of Thermally Activated Delayed  
6  
7 Fluorescence. *Nat. Commun.* **2016**, *7*, 13680.  
8  
9  
10  
11  
12  
13  
14  
15  
16  
17  
18  
19  
20  
21  
22  
23  
24  
25  
26  
27  
28  
29  
30  
31  
32  
33  
34  
35  
36  
37  
38  
39  
40  
41  
42  
43  
44  
45  
46  
47  
48  
49  
50  
51  
52  
53  
54  
55  
56  
57  
58  
59  
60

1  
2  
3  
4  
5  
6  
7  
8  
9  
10  
11  
12  
13  
14  
15  
16  
17  
18  
19  
20  
21  
22  
23  
24  
25  
26  
27  
28  
29  
30  
31  
32  
33  
34  
35  
36  
37  
38  
39  
40  
41  
42  
43  
44  
45  
46  
47  
48  
49  
50  
51  
52  
53  
54  
55  
56  
57  
58  
59  
60